Powner, M. B., McKenzie, J. A. G., Christianson, G. J., Roopenian, D. C. & Fruttiger, M. (2014). Expression of neonatal Fc receptor in the eye. Physiology and Pharmacology, 55(3), pp. 1607-1615. doi: 10.1167/iovs.13-12574

Expression of Neonatal Fc Receptor in the Eye

Michael B. Powner,[1] Jenny A. G. McKenzie,[1] Gregory J. Christianson,[2] Derry C. Roopenian,[2] and Marcus Fruttiger[1]

[1]UCL Institute of Ophthalmology, University College London, London, United Kingdom
[2]The Jackson Laboratory, Bar Harbor, Maine

Correspondence: Marcus Fruttiger, UCL Institute of Ophthalmology, University College London, London EC1V 9EL, United Kingdom; m.fruttiger@ucl.ac.uk.

Submitted: June 10, 2013
Accepted: February 4, 2014

Citation: Powner MB, McKenzie JAG, Christianson GJ, Roopenian DC, Fruttiger M. Expression of neonatal Fc receptor in the eye. *Invest Ophthalmol Vis Sci*. 2014;55:1607–1615. DOI:10.1167/iovs.13-12574

Purpose. The neonatal Fc receptor (FcRn) plays a critical role in the homeostasis and degradation of immunoglobulin G (IgG). It mediates the transport of IgG across epithelial cell barriers and recycles IgG in endothelial cells back into the bloodstream. These functions critically depend on the binding of FcRn to the Fc domain of IgG. The half-life and distribution of intravitreally injected anti-VEGF molecules containing IgG-Fc domains might therefore be affected by FcRn expressed in the eye. In order to establish whether FcRn–Fc(IgG) interactions may occur in the eye, we studied the mRNA and protein distribution of FcRn in postmortem ocular tissue.

Methods. We used qPCR to study mRNA expression of the transmembrane chain of FcRn (FCGRT) in retina, optic nerve, RPE/choroid plexus, ciliary body/iris plexus, lens, cornea, and conjunctiva isolated from mouse, rat, pig, and human postmortem eyes and used immunohistochemistry to determine the pattern of FcRn expression in *FCGRT*-transgenic mouse and human eyes.

Results. In all four tested species, *Fcgrt* mRNA was expressed in the retina, RPE/choroid, and the ciliary body/iris, while immunohistochemistry documented FcRn protein expression in the ciliary body epithelium, macrophages, and endothelial cells in the retinal and choroidal vasculature.

Conclusions. Our results demonstrate that FcRn has the potential to interact with IgG-Fc domains in the ciliary epithelium and retinal and choroidal vasculature, which might affect the half-life and distribution of intravitreally injected Fc-carrying molecules.

Keywords: blood-ocular barrier, drug delivery, ciliary epithelium, macrophages

The neonatal Fc receptor (FcRn) is a heterodimer composed of a transmembrane alpha chain (FCGRT) and a soluble beta chain (beta-2-microglobullin, B2M).[1] This heterodimer plays a critical role in the homeostasis of albumin and immunoglobulin G (IgG) by regulating intracellular trafficking of these proteins in epithelial cells, the vascular endothelium, and inflammatory cells.[2–5] The function of FcRn was first recognized in the neonatal rodent intestine, where it mediates the transfer of maternal IgG to the newborn.[6]

In adult physiology, FcRn is important for the maintenance of albumin and IgG levels in the plasma. This was most convincingly demonstrated in mice lacking a functional *Fcgrt* gene, which had reduced albumin and IgG levels in the plasma compared with wild-type controls.[2] The mechanism of this protective effect is based on FcRn localized in early endosomes in endothelial cells. IgG may be incorporated into endothelial endosomes by nonspecific endocytosis of soluble extracellular material. The Fc domain of IgG is then bound by FcRn in acidic early endosomes in a strictly pH-dependent manner.[7] This leads to recycling of the IgG to the cell surface where, facilitated by neutral pH, IgG is released again. This IgG-Fc specific salvaging mechanism is the reason why the half-life of IgG in plasma is greatly extended compared with that of other antibody classes.[8,9] The interest in mechanisms that influence IgG half-life and transport has been heightened by the emergence of monoclonal IgG antibodies as useful therapeutic agents.

In the ophthalmic clinic, VEGF-blocking antibodies are routinely injected into the vitreous. They are effective in halting the progression of AMD with choroidal neovascularization or exudative forms of AMDs and in the treatment of exudative forms of central or branch retinal vein occlusion or thrombosis, as well as in the treatments of some forms of diabetic retinopathy edemas, and are currently also in trial for other eye conditions with vascular complications. However, the retina is an immune privileged site and immunoglobulins are normally excluded by the retina-blood-barrier. The high concentration of IgG after intravitreally injection is therefore not a naturally occurring situation and the biological mechanisms that affect the fate of intravitreally injected antibodies are not well understood. The topic is clinically relevant not only for the therapeutic effects of anti-VEGF antibodies within the eye, but also for off-target effects in the periphery if anti-VEGF antibodies are transported from the vitreous into the blood circulation.

Since FcRn transports IgG across epithelial and endothelial barriers, it is plausible that FcRn-mediated mechanisms exert control over the distribution and persistence of intravitreally injected therapeutic IgG. Defining the cellular patterns of FcRn expression in the substructures of the eye is therefore clinically relevant. However, such information is currently limited to a previous study of rat ocular tissue in which a monoclonal antibody was used to localize FcRn to the ciliary body and retinal blood vessels but not to the RPE and choroid.[10] Here we

address this issue more comprehensively by using a combination of RT-qPCR and immunohistochemistry to define the patterns of FcRn expression in substructures of the rat, mouse, pig, and human eyes.

Materials and Methods

mRNA Isolation

Tissue samples of unfixed retina, RPE/choroid complex, optic nerve, iris/ciliary body, lens, cornea, and conjunctiva were dissected from rats ($n = 3$); C57BL/6J mice ($n = 3$); and pig ($n = 3$) eyes, and snap-frozen ready for RNA extraction. Three sets of samples were also dissected from equivalent regions from two anonymous human eye donors. The human tissue did not include corneas as these were used for transplantation. Isolated samples were snap-frozen on dry ice. For mouse endothelial cell–enriched samples, five mouse retinas were pooled and enzymatically digested. Endothelial cells were isolated using magnetic beads (Dynabead; Invitrogen, Carlsbad, CA) as previously described.[11] Isolated endothelial cells and leftover retinal cells were then snap-frozen. Three independent experiments were performed and results averaged. For human RPE enrichment, three separate regions of RPE/choroid complex were dissected from two donor eyes. The RPE was separated from the choroid by gently pipetting 50 μL RNase free PBS over the surface until no RPE cells were left visible under a dissection microscope. The RPE cells suspended in PBS and the remaining choroid were then snap-frozen. RNA was extracted from the collected samples using a commercial reagent (TRIzol; Sigma-Aldrich, St. Louis, MO) and cDNA was reverse-transcribed using a reverse transcription kit (Qiagen QuantiTect; Qiagen, Venlo, Limburg). Three independent experiments were performed and results averaged.

Quantitative Real-Time PCR (qPCR)

Real-time PCR was performed using a master mix (GoTag qPCR; Promega, Madison, WI) and the following primer pairs:

1. Rat—*β-actin (Actb)* F: AAGATCAAGATCATTGCTCCTCC R: TAACAGTCCGCCTAGAAGCA, *Gapdh* F: GA GAAACCTGCCAAGTATGATGAC R: GGGAGTTGCTGTT GAAGTCAC, *CyclophilinA (Ppia)* F: CCAAACA CAAATGGTTCCCAG R: CCCGCAAGTCAAAGAAA TTAGAG, *Fcgrt* F: CCAGGTGTCTTGGTATTGGG R: GTGTGAAGGTCCCATTTATTTGGT;
2. Mouse—*Actb* F: TCCAAGTATCCATGAAATAAGTGG R: GCAGTACATAATTTACACAGAAGC, *Gapdh* F: GA GAAACCTGCCAAGTATGATGAC R: ATCGAAGGTGGAA GAGTGGG, *Ppia* F: ACTTCATCCTAAAGCATACAGGTC R: CTTGCCATCCAGCCATTCAG, *Fcgrt* F: AGCT CAAGTTCCGATTCCTG R: GATCTGGCTGATGAATC TAGGTC, *Cdh5* F: TGGAAACACAAGATGCCCTG R: TGTATGTGGATTGAGTAAAGACGG;
3. Pig—*Actb* F: ATCCTGACCCTCAAGTACCC R: AGAGTC CATGACAATGCCAG, *Gapdh* F: CATCAAGAAGGTGGT GAAGCAG R: TTCATTGTCGTACCAGGAAATGAG, *Ppia* F: AAGACTGAGTGGTTGGATGG R: AATGGT GATCTTCTTGCTGGT, *Fcgrt* F: GTCGTCGCTAACAGTC AAGAG R: CCACGATCAAGAGCAGTAGGA; and
4. Human—*Actb* F: CCTGGACTTCGAGCAAGAGATG R: AGGAAGGAAGGCTGGAAGAGTG, *GAPDH* F: CATCAA GAAGGTGGTGAAGCAG R: TTCATTGTCGTACCAG GAAATGAG, *PPIA* F: AAGACTGAGTGGTTGGATGG R: AATGGTGATCTTCTTGCTGGT, *FCGRT* F: GAAACCTG GAGTGGAAGGAG R: CGGAGGGTAGAAGGAGAAGG and *RPE65* F: AAGATGATGGTGTAGTTCTGAGTG R: AAGGTGACAGGGATGTTAATCTC.

Each sample was measured in triplicates in three separate experiments based on *Actb*, *Gapdh*, and *Ppia* internal controls. Relative values based on the three different internal controls were all similar and averaged. Three samples per tissue type were measured in this way and then averaged.

Tissue for Immunohistochemistry

In the case of mice and rats, whole eyes were removed, placed in OCT compound, and flash-frozen. Alternatively, the cornea was pierced and the eyes were fixed in 4% (wt/vol) paraformaldehyde (PFA, Sigma-Aldrich) in PBS for 1 hour at room temperature (RT), equilibrated in 30% (wt/vol) sucrose (Sigma-Aldrich) in PBS, transferred to, and orientated in OCT compound (Agar Scientific, Essex, UK) and frozen. Mouse strains used were C57BL/6J, *Fcgrt* knockout mice B6.Cg-*Fcgrt*^{tm1Dcr} (*Fcgrt*$^{-/-}$),[12] and B6.Cg-*Fcgrt*^{tm1Dcr} Tg(FCGRT)32Dcr/DcrJ, which carry a human *FCGRT* transgene and lack mouse *Fcgrt* (*hFCGRT* transgenic mice).[13]

Human eyes collected by Moorfields Eye Bank for corneal transplantation from anonymous donors were dissected to isolate samples from the ciliary body, iris, lens, and a region of posterior pole containing optic nerve, parafovea, and temporal retina. Tissue was either flash-frozen unfixed or alternatively fixed in 2% (wt/vol) PFA, equilibrated in 30% (wt/vol) sucrose in PBS and frozen in OCT compound.

Immunohistochemistry

Cryosections (10 μm) were cut from mouse and human samples, mounted on slides (Superfrost Plus; VWR, Leicestershire, UK), and left to dry at RT. Cryosections from unfixed tissue were fixed in acetone (Sigma-Aldrich) for 10 minutes at −20°C prior to further processing. For IBA-1 staining, adjacent sections from unfixed tissue were fixed with 4% (wt/vol) PFA for 10 minutes prior to further processing. Sections from PFA-fixed human tissue required antigen retrieval prior to IHC; sections were heated to 110°C in a solution of 90% glycerol and 10% 0.01 M citrate buffer, pH 6.0 for 10 minutes. Sections were then incubated in blocking buffer (1% [wt/vol] bovine serum albumin, 0.5% [wt/vol] Tween20 in PBS, all reagents from Sigma-Aldrich) for 1 hour at RT, followed by 1 hour at RT in primary antibodies diluted in blocking buffer. Sections were treated in wash buffer (0.5% [wt/vol] Tween20 in PBS) and incubated in secondary antibody diluted in wash buffer for 1 hour at RT. Sections were then treated with wash buffer, counter stained with Hoechst, washed with PBS, mounted in mounting medium (Mowiol 4-88; Merck Millipore, Billerica, MA) and imaged with a confocal microscope (Zeiss LSM 700; Carl Zeiss Microscopy, Thornwood, NY).

Primary antibodies used for hFcRn detection were rabbit, polyclonal anti-FCGRT, Human Protein Atlas[14] (HPA)012122 (Sigma-Aldrich); HPA015130 (Sigma-Aldrich); M-255 (sc-66893; Santa Cruz Biotechnology, Dallas, TX); H-274 (sc-66892, Santa Cruz Biotechnology); mouse, monoclonal anti-FCGRT, 1G3 (myeloma hybridoma cell line CRL-2434); H-4 (sc-166413; Santa Cruz Biotechnology); and ADM31.[15] Iba-1 antibody (rabbit) was used as a macrophage marker.[16] Secondary antibodies (Invitrogen) used were goat AlexaFluor 594-conjugated anti-mouse IgG, donkey AlexaFluor 555-conjugated anti-rabbit IgG, rabbit anti-mouse IgG, and rabbit anti-AlexaFluor 488. Lectins used were fluorescein conjugated IB4 (Vector Labs, Burlingame, CA) for mouse and fluorescein conjugated UAE (Sigma-Aldrich) for human tissue. Conjugation

Investigative Ophthalmology & Visual Science

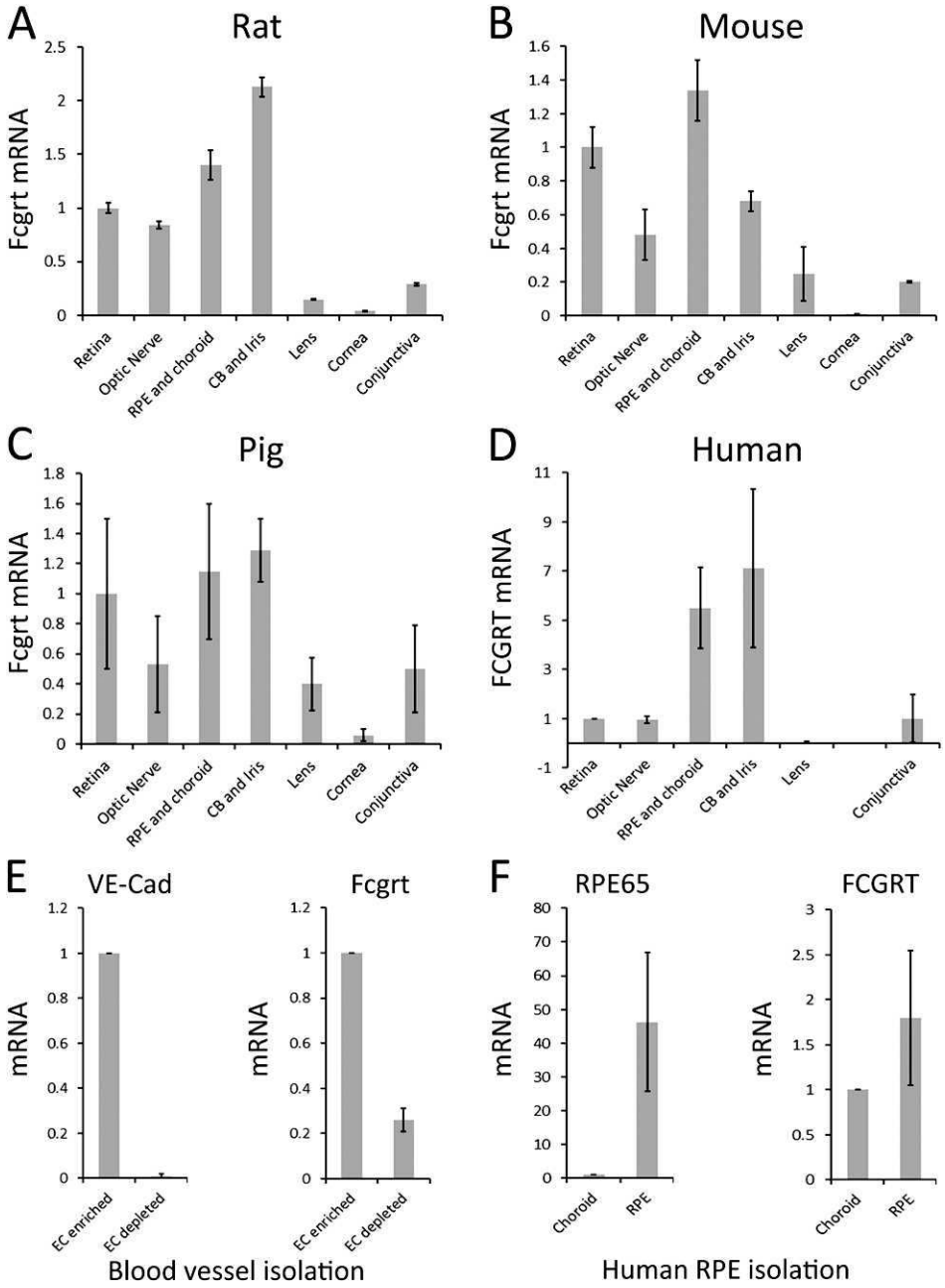

Figure 1. Fcgrt mRNA levels in different tissues of the eye measured by RT-qPCR. Values were normalized to 3 internal standards (*Actb*, *Gapdh*, and *Ppia*) and averaged. (**A–D**) Measurements in different tissues isolated from rat, mouse, pig, and human eyes (three samples from each tissue in each species). They have been normalized to retina values. (**E**) qPCR measurements on dissociated mouse retina after bead-based enrichment of blood vessel fragments from three independent experiments. The *left panel* demonstrates enrichment efficiency using an endothelial cell marker (cadherin 5, also known as VE-Cad) and the *right panel* shows *Fcgrt* mRNA levels. (**F**) Shows in the *left panel* an RPE-specific marker (RPE65) to demonstrate efficiency of RPE cell enrichment from human choroid. The *right panel* shows an enrichment of *FCGRT* mRNA in the RPE fraction (three independent experiments). *Error bars* indicate standard deviations based on the variations between the three samples.

of antibodies with AlexaFluor 488 was carried out using an antibody labeling kit (APEX; Invitrogen) according to the manufacturer's instructions.

Results

Fcgrt mRNA Expression in the Eye

To assess where in the eye FcRn is present, we used RT-qPCR to measure *Fcgrt* mRNA in tissue that had been dissected from different parts of the eye. Species-specific primers for *Fcgrt* from four different species (mouse, rat, pig, and human) were used. Values were internally normalized against mRNA from three different housekeeping genes (*Actb, Gapdh,* and *Ppia*) from the same sample. From different species and different tissue types, three samples each were measured and averaged (Fig. 1). In the rat eye (Fig. 1A), *Fcgrt* mRNA was readily detected in the retina, optic nerve, RPE/choroid, and ciliary body/iris. Expression in the lens, cornea, and conjunctiva was much lower. Very similar findings were made in mouse and pig eyes (Figs. 1B, 1C). In all of these three species expression was

Investigative Ophthalmology & Visual Science

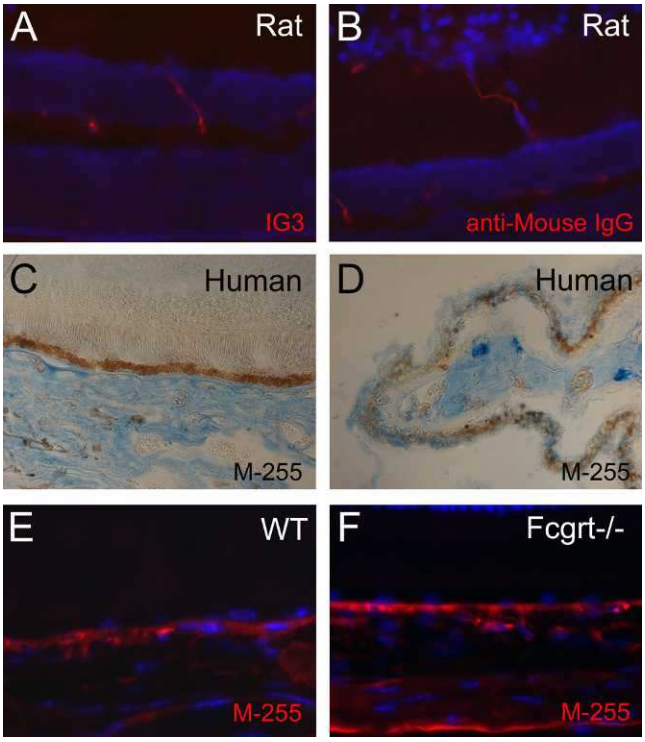

Figure 2. IG3 and M-255 antibodies fail to specifically detect FcRn by immunohistochemistry. Immunohistochemistry with the mouse monoclonal IG3 antibody (anti-FcRn, *red* in [**A**]) appears the same as the negative control with only secondary antibody (anti-mouse IgG, *red* in [**B**]). The polyclonal rabbit M-255 antibody (anti-FcRn) provided staining on human choroid (**C**) and ciliary body (**D**). However, a similar staining pattern was obtained in choroid from wild-type (WT) mice (**E**) and FcRn knockout (Fcgrt$^{-/-}$) mice (**F**), suggesting nonspecific activity of the M-255 antibody.

lowest in the cornea. In human eyes (Fig. 1D), we did not obtain a sample from the cornea because the postmortem eye donations we used for our analysis were for the primary purpose of corneal transplantation. In the other human samples, we found particularly high expression of *FCGRT* mRNA in the RPE/choroid and the ciliary body/iris.

We then applied cell enrichment protocols prior to mRNA isolation to investigate the cell patterns of *Fcgrt* expression. To this end, antibody-coated magnetic beads were used to isolate endothelial cells from single cell suspensions of mouse retinas. This resulted in a 60-fold enrichment of mRNA for the endothelial cell marker cadherin 5 (Cdh5, also known as VE-cadherin) in the endothelial cell–enriched fraction versus the remaining endothelial cell–depleted retinal cells (Fig. 1E). *Fcgrt* mRNA was also enriched in the endothelial fraction (5-fold), demonstrating that the majority of *Fcgrt* mRNA in the retina is expressed by endothelial cells. However, *Fcgrt* mRNA was not enriched to the same extent as *Cdh5* mRNA, which could suggest that some nonendothelial cells in the mouse retina also express *Fcgrt*.

For the human RPE/choroid sample, we used a mechanical fractionation method based on pipetting buffer over the surface of the RPE/choroid plexus to peel the RPE cells. The RPE marker RPE65 was approximately 50 times enriched in the RPE fraction, demonstrating efficient separation of the two fractions. *FCGRT* mRNA was increased about 2.5-fold in the isolated RPE cells (Fig. 1F), suggesting that *FCGRT* mRNA is expressed by RPE cells. Furthermore, the signal in the choroid fraction suggests that also cells in the choroid plexus express *FCGRT* mRNA.

Nonspecificity Immunohistochemistry Staining of Anti-hFcRn Antibodies

In order to establish the spatial distribution of hFcRn by IHC, we tested a panel of reagents reported to provide antigen-specific staining patterns. To this end we used cryosections from PFA-fixed tissue and cryosections from unfixed, snap-frozen tissue, post-fixed on the slide with acetone. We tested six different commercially available antibodies that have been reported to be suitable for hFcRn detection by IHC.[10,14,17] Two antibodies (polyclonal rabbit anti-FCGRT, HPA012122 and HPA015130) failed to provide any signal on cryosections from human, mouse, or rat eyes with either fixation method (not shown). A third antibody (mouse monoclonal 1G3) also failed to stain human tissue (not shown). On rat tissue, this antibody stained retinal blood vessels nonspecifically (Figs. 2A, 2B), presumably due to cross-reactivity of secondary anti-mouse IgG antibodies with endogenous rat IgG.

In contrast, two further antibodies (rabbit polyclonal H-275 and M-255) both revealed a very similar, strong staining on human tissue in the choroid plexus, the ciliary body (shown for M-255 in Figs. 2C, 2D) and large retinal vessels (not shown), which was consistent with our qPCR expression data (Fig. 1). On mouse tissue, these antibodies (H-275 and M-255) also produced a similar result, staining the choroid, retinal vessels (shown for M-255 in Fig. 2E) and the ciliary body (not shown). However, positive staining appeared to be diffuse and not associated with specific cell populations (Figs. 2C, 2D). Furthermore, an identical staining pattern was observed for eyes from *Fcgrt* knockout (*Fcgrt*$^{-/-}$) mice with antibody M-255 (Fig. 2F) and antibody H-275 (not shown). We therefore concluded that neither of these two polyclonal antibodies was suitable for reliable FcRn detection of eye tissue by IHC.

Specific IHC Staining of FCGRT in Transgenic Mice

We also tested a mouse monoclonal anti-hFcRn antibody (ADM31) that was generated by immunizing *Fcgrt*$^{-/-}$ mice with spleen cells from mice that overexpress human *FCGRT*.[15,18] The antibody is reported to react only with hFcRn and not with the orthologous mouse heterodimer.[15] In order to further evaluate this antibody, we used human (h) *FCGRT* transgenic mice (line 32) that lack the mouse *Fcgrt* gene (*hFCRN* transgenic mice).[13] Furthermore, to overcome the problem of secondary anti-mouse antibodies cross-reacting with endogenous mouse IgG, we directly conjugated ADM31 antibody with AlexaFluor 488. This did not result in a directly observable staining. However, signal amplification via the use of a rabbit antibody against AlexaFluor 488 and subsequent detection with a donkey anti-rabbit IgG AlexaFluor 596-conjugated antibody resulted in strong staining in tissues from *hFCGRT* transgenic mice. The strongest signal was visible in the ciliary body and choroid plexus, with weaker staining also visible in the retinal vasculature (Figs. 3A, 3D, 3G, 3J, 3M, 3P). Only acetone-fixed sections could be stained, whereas PFA-fixed tissue did not yield any staining. Eye tissue from *Fcgrt*$^{-/-}$ mice was not labeled (Figs. 3B, 3E, 3H, 3K, 3N, 3Q), confirming the specificity of the ADM31 antibody. Tissue from wild type *Fcgrt*$^{+/+}$ mice was not labeled either (Figs. 3C, 3F, 3I, 3L, 3O, 3R), which was expected since the ADM31 antibody does not bind mouse FcRn.

FcRn Immunohistochemistry of Human Eyes

Having established the specificity of the ADM31 antibody in detecting hFcRn by IHC in *hFCGRT* transgenic mice, we used this antibody to study the distribution of hFcRn on acetone-fixed sections from human eyes. In this instance, we used

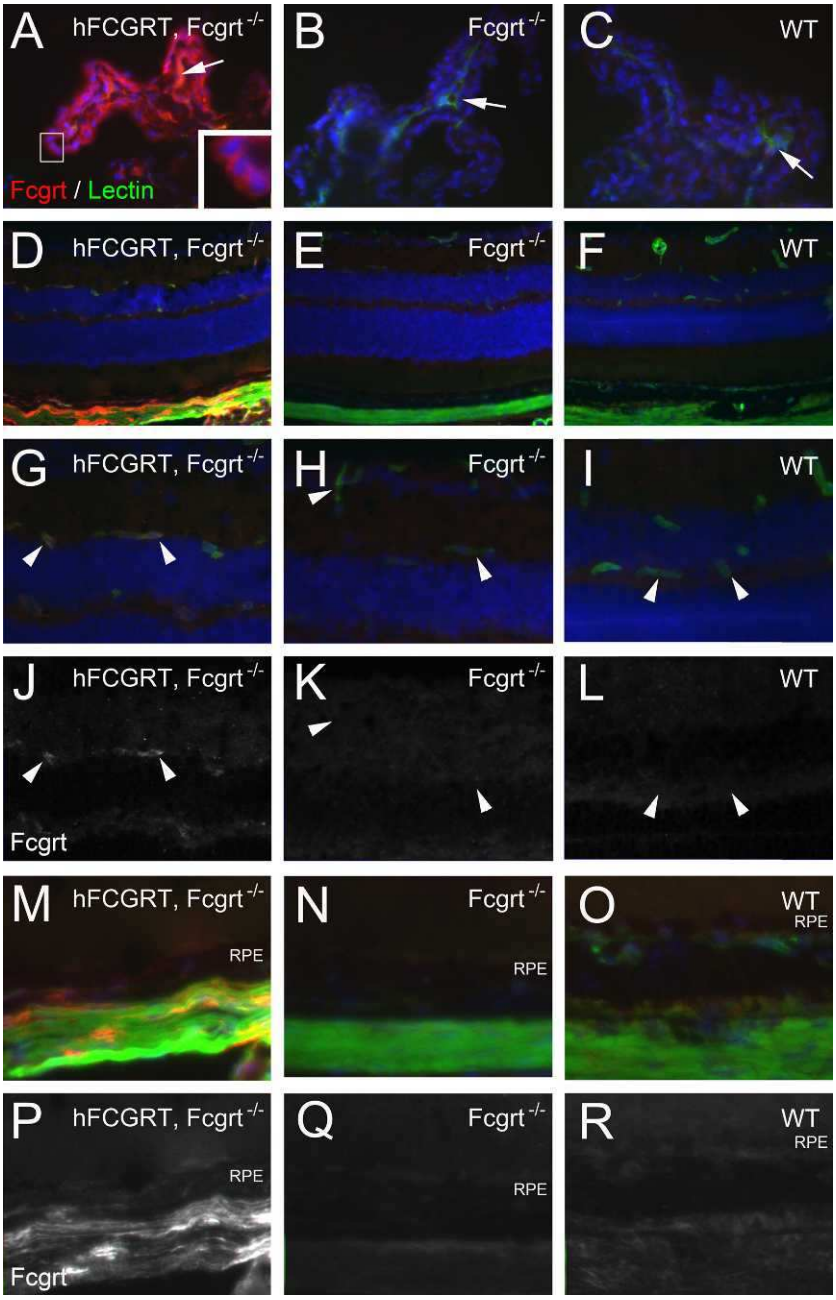

Figure 3. hFcRn in *hFCGRT*-transgenic mouse eyes (*red* in [**A–I**, **M–O**] and *white* in [**J–L**, **P–R**]). Blood vessels have been stained with lectin (IB4, *green* in [**A–I**, **M–O**]). Transgenic mice expressing human hFcRn are shown in (**A**, **D**, **G**, **J**, **M**, **P**); mice lacking *Fcgrt* are shown in (**B**, **E**, **H**, **K**, **N**, **Q**); and wild-type mice are in (**C**, **F**, **I**, **L**, **O**, **R**). Ciliary body is shown in (**A–C**); retina and choroid in (**D–F**); retinal vasculature capillaries (*arrowheads*) in (**G–L**) and choroid in (**M–R**). *Arrows* in (**A–C**) indicate blood vessels.

rabbit anti-mouse IgG and AlexaFluor 596 donkey anti-rabbit IgG to visualize ADM31 binding.

Prominent staining was found in the ciliary body (Figs. 4A–C). The nonpigmented ciliary body epithelium was particularly strongly labeled. In the pigmented ciliary body, the signal seemed weaker (Figs. 4D–F), which may have been caused partly through quenching of the fluorescent signal by the pigment. At higher magnification the staining appeared vesicular (Figs. 4G–I), consistent with the known cellular location of FcRn in endosomes. Blood vessels in the ciliary body were not stained (Figs. 4J–L). This was in contrast to our findings in the transgenic mice, where blood vessels in the ciliary body were strongly stained (Fig. 3A). In addition, strongly labeled, isolated cells were detected in the ciliary body stroma (Figs. 4J–L), which are most likely immune cells, such as macrophages (see below).

In the choroid (Fig. 5) we also found strongly hFcRn positive, single cells (arrowheads in Figs. 5A–I). They were often in a perivascular location. In order to establish the identity of these cells, we used a marker for resident macrophages (Iba1).[16] The acetone fixation (required for the hFcRn staining) prevented colabeling with Iba1 and we therefore used PFA-fixed adjacent sections. The distribution of Iba-1 positive cells was similar and in some instances cells could be detected in similar locations in both sections (arrowheads in Figs. 5G–L).

Investigative Ophthalmology & Visual Science

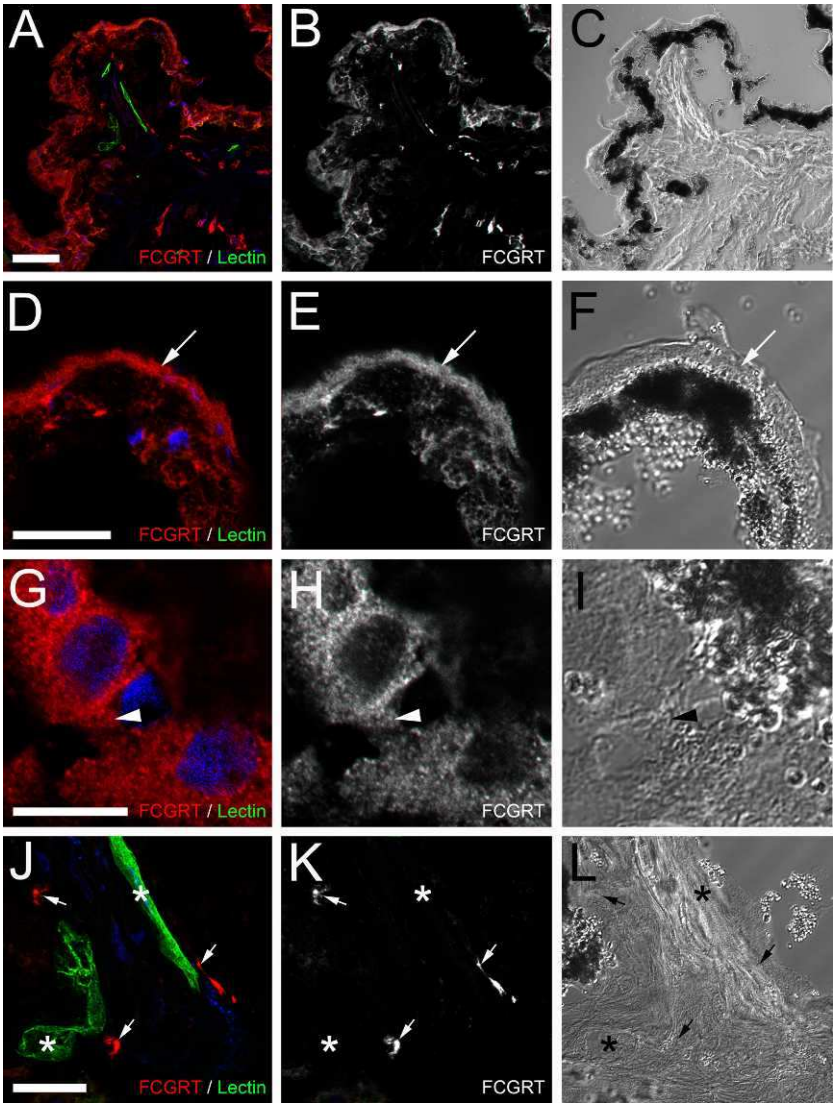

Figure 4. FcRn expression in the human ciliary body. Fluorescent immunohistochemistry with ADM31 antibody visualizes the distribution of FcRn (*red* in [**A**, **D**, **G**, **J**] and *white* in [**B**, **E**, **H**, **K**]) in the ciliary body. Blood vessels (*stars* in [**J**, **K**, **L**]) are labeled with lectin (UAE) in *green* (**A**, **D**, **G**, **J**). Bright field images are shown in (**C**, **F**, **I**, **L**). *Arrows* in (**D**–**F**) indicate the nonpigmented ciliary epithelium. High magnification reveals a punctate stain in nonpigmented ciliary epithelium (*arrowheads* in [**G**–**I**]). In the ciliary body stroma, strongly FcRn-positive cells can be detected (*arrows* in [**J**–**L**]) but blood vessels (*stars* in [**J**–**L**]) are negative. *Scale bars* are 50 μm in (A), 20 μm in (D, J), and 10 μm in D.

Blood vessels were hFcRn positive in the choriocapillaris (arrows in Figs. 5D–F), but larger vessels in Sattler's and Haller's layer were negative (star in Figs. 5G–I). In the retinal vasculature (Fig. 6), we found an inverse situation; here the large vessels were hFcRn positive (Figs. 6A–F) but not capillaries (Figs. 6M–O). As in the choroid, in the retina were also numerous, strongly hFcRn-positive perivascular cells (arrowheads in Figs. 6A–I, M–O). Iba1 immunohistochemistry in an adjacent section (Figs. 6J–L) strongly suggests that these perivascular cells are macrophages.

Discussion

In this study we describe FcRn expression in three main locations: the ciliary body epithelium, macrophages, and endothelial cells of the choroid and retinal vasculature.

Our RT-qPCR analysis revealed similar expression of *Fcgrt* mRNA in the RPE/choroid and the ciliary body/iris plexus in four different species (rat, mouse, pig, and human). A further commonality between rat, mouse, and pig was very low expression in the cornea (human cornea was not measured). These findings partially conflict with a previous study based on semiquantitative PCR procedures that reported a complete absence of *Fcgrt* mRNA in rat RPE/choroid, low levels in the ciliary body/iris, and high levels in the cornea.[10] The discrepancies might be explained by the different methods used to measure *Fcgrt* mRNA. Semiquantitative PCR can be affected by differences in the efficiency of mRNA isolation, reverse transcription, and loading volumes. We used qPCR techniques and three separate internal standards (*Actb*, *Gapdh*, and *Ppia*) to normalize our data, which should provide a more accurate representation of gene expression.

Our RT-qPCR findings were largely confirmed by immunohistochemistry on human and transgenic mouse tissue. We have gone to great lengths to ensure that our hFcRn immunohistochemistry was specific. Surprisingly, the commercially available antibodies we tested either provided no or nonspecific signals. In contrast, specificity of the ADM31

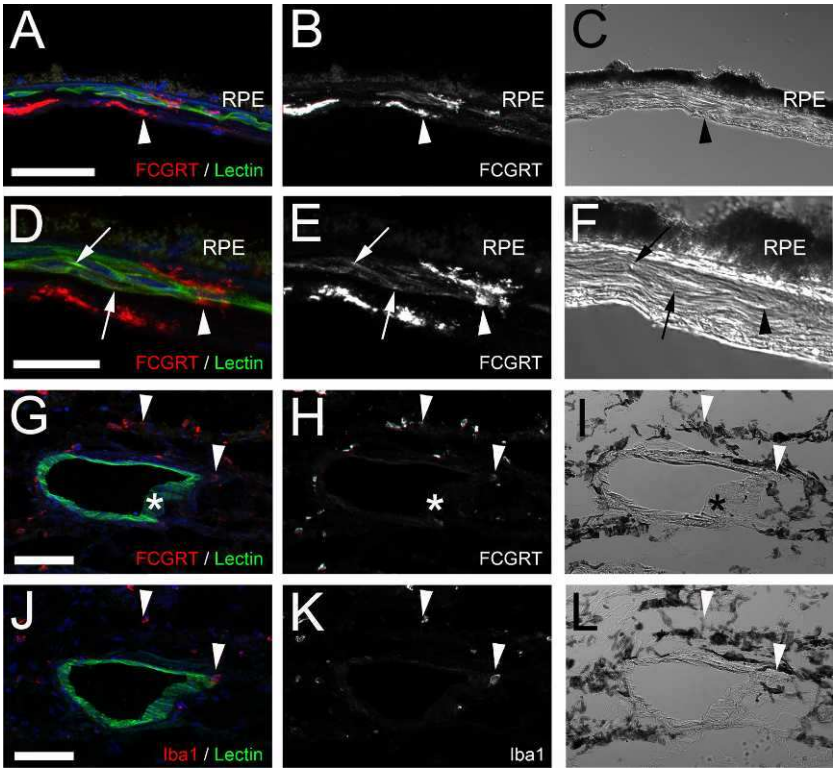

Figure 5. FcRn expression in the human choroid. Fluorescent immunohistochemistry with ADM31 antibody visualizes the distribution of FcRn (*red* in [**A**, **D**, **G**] and *white* in [**B**, **E**, **H**]) in the choroid. Macrophages (*arrowheads*) are labeled with Iba1 antibody (*red*) in (**J**) and (*white*) (**K**) in an adjacent section. Blood vessels are labeled with lectin in *green* (**A**, **D**, **G**, **J**). Bright field images are shown in (**C**, **F**, **I**, **L**). *Arrows* in (**D**–**F**) indicate FcRn-positive endothelial cells in the choriocapillaris. Large vessels (*star* in [**G**, **H**]) are FcRn negative. *Scale bars* are 50 μm in (A, G, J) and 20 μm in (D).

antibody for human hFcRn was clearly demonstrated in our study by positive staining in *hFCGRT* transgenic mice and the absence of staining in *FcRn*$^{-/-}$ mice.

Expression of hFcRn in transgenic mice was highest in the ciliary body epithelium and in the RPE/choroid plexus. This matched our IHC and qPCR data from human tissue. The transgene used for the generation of the transgenic mice was a 33-kb cosmid clone including the entire *FCGRT* gene (approximately 11 kb) as well as 10 kb of 5′ and 3′ flanking sequences, which is likely to confer good replication of endogenous hFcRn expression. Ongoing studies indicate that the tissue patterns of hFcRn expression determined by ADM31 are consistent with those generally expected in humans (Roopenian et al; unpublished observations, 2013); however, definition of the tissues sites of FCGRT expression in humans is blurred by the issues raised above concerning the reliability of many antibodies commonly used for detection. The differential patterns of hFcRn observed in ciliary stromal vessels found in human and transgenic mice using the highly specific antibody ADM32 remains to be explained.

In human tissue, hFcRn immunohistochemistry and qPCR data matched surprisingly well. Both readouts detected strong expression in the ciliary body epithelium and in the RPE/choroid and relatively low expression in the retina. This consistency across different measurement techniques provides further confidence into the reliability of our results.

FcRn has a known function in endothelial cells.[5,19] Our finding of FcRn-positive endothelial cells in the choriocapillaris and large retinal vessels is consistent with this site of action. However, capillaries in the retinal vasculature and large vessels in the choroid lacked staining. In our study, it is not clear whether the absence of staining in certain vessels is due to a complete lack of expression or due to low expression levels below the detection limit of our immunohistochemistry. However, it has been shown previously that endothelial FcRn expression can vary considerably in different vascular beds,[5] underscoring the heterogeneity of the endothelium.

Immunohistochemistry on RPE of human tissue sections was inconclusive. A previous study has reported *FCGRT* mRNA in primary cultures of human RPE cells.[20] Our qPCR data on isolated human RPE cells (Fig. 1G) supports this finding. However, on tissue sections, a potential FcRn immunohistochemistry signal was below the detection limit and could not be distinguished from autofluorescence in human RPE.

In contrast, we found very strong FcRn staining on many single, isolated cells in the choroid and the ciliary body stroma and in the retina. These cells were often found in a perivascular location and are most likely monocytic antigen-presenting cells, which are known to express high levels of FcRn.[5,21] This may be particularly relevant in AMD patients who are injected with VEGF-blocking molecules containing an intact IgG-Fc domain. AMD is known to be driven at least in part by inflammatory components, such as macrophages,[22–24] which might influence the pharmacokinetics of IgG-Fc containing molecules.

FcRn staining was also very strong in the ciliary body epithelium, but the biological significance of FcRn at this site is not clear. One of the main functions of the ciliary body is to produce aqueous humor from blood. The concentration of IgG in aqueous humor is more than 100 times lower than in blood.[25] FcRn in the ciliary body might therefore be responsible for retaining IgG in the blood. It is also possible that, like in endothelial cells, FcRn protects IgG from degradation in ciliary body epithelium. In addition, FcRn might

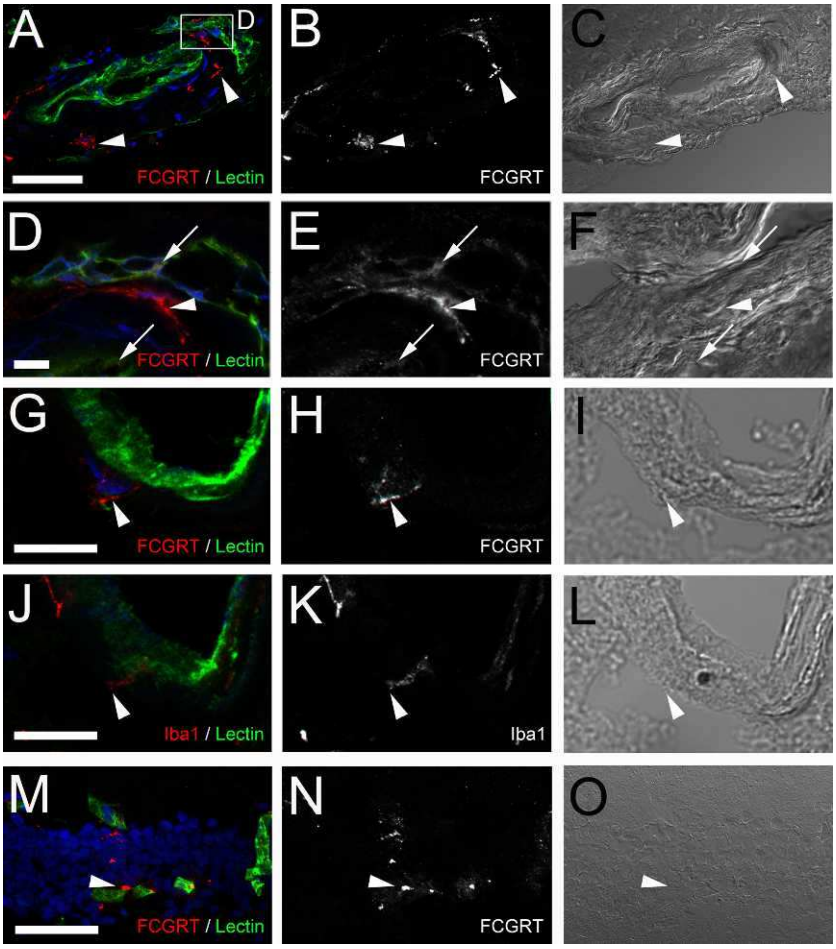

Figure 6. FcRn expression in the human retina. Fluorescent immunohistochemistry with ADM31 antibody visualizes the distribution of FCGRT (*red* in [**A**, **D**, **G**, **M**] and *white* in [**B**, **E**, **H, N**]) in the retina. Iba1 antibody visualizes macrophages in *red* (**J**) and *white* (**K**) in an adjacent section. Blood vessels are labeled with lectin in *green* (**A**, **D**, **G**, **J**, **M**). Bright field images are shown in (**C**, **F**, **I**, **L, O**). (**A–C**) shows a large vessel in the retina with strongly FCGRT-labeled perivascular cells (*arrowheads*). Higher magnification of this vessel ([**D–F**], indicated by the white box in [**A**]) also shows FCGRT-positive endothelial cells (*arrows*). A strongly FcRn-positive, perivascular cell (*arrowheads* in [**G–I**]) is Iba1 positive in an adjacent section (*arrowheads* in [**J–L**]). Capillaries in the retina are FcRn negative (**M–O**). *Scale bars* are 50 μm in (**A**, **M**) and 10 μm in (**D**, **F**).

also mediate reverse transcytosis, the transport of IgG from the CNS/retina into the blood stream. In the brain, this occurs in the choroid plexus, where FcRn has been shown to be expressed.[5,17] It has been suggested that this process is responsible for the rapid removal of therapeutic IgG injected into the brain.[26,27] A similar mechanism might also apply to the ciliary body.

Several studies have shown prolonged reduction of VEGF in the systemic circulation of patients after intravitreal injection of bevacizumab (an anti-VEGF antibody containing an IgG-Fc domain).[28–31] This clearly demonstrates that intravitreally injected IgG can cross the blood-retina barrier. In contrast, systemic plasma concentrations of VEGF were not affected by intravitreal ranibizumab (an anti-VEGF Fab fragment, lacking an Fc domain).[28,30] This could be explained by the different half-lives in plasma of the two anti-VEGF agents.[8,9] However, it is also possible that FcRn in the eye might contribute to an IgG-Fc specific transport mechanism from the eye into the periphery.

In summary, our study has shown that FcRn is expressed in several locations in the eye where potential interactions between FcRn and intravitreally injected molecules containing IgG-Fc domains can occur, which might affect their local distribution, half-life in the eye and transport into the peripheral circulation.

Acknowledgments

Supported by a UCL–Industry Research Collaboration funded by Novartis.

Disclosure: **M.B. Powner**, Novartis (R); **J.A.G. McKenzie**, None; **G.J. Christianson**, The Jackson Laboratory (E); **D.C. Roopenian**, The Jackson Laboratory (E), P; **M. Fruttiger**, Novartis (F, C)

References

1. Simister NE, Mostov KE. An Fc receptor structurally related to MHC class I antigens. *Nature*. 1989;337:184–187.
2. Chaudhury C, Mehnaz S, Robinson JM, et al. The major histocompatibility complex-related Fc receptor for IgG (FcRn) binds albumin and prolongs its lifespan. *J Exp Med*. 2003;197:315–322.
3. Ward ES, Zhou J, Ghetie V, Ober RJ. Evidence to support the cellular mechanism involved in serum IgG homeostasis in humans. *Int Immunol*. 2003;15:187–195.
4. Roopenian DC, Akilesh S. FcRn: the neonatal Fc receptor comes of age. *Nat Rev Immunol*. 2007;7:715–725.
5. Akilesh S, Christianson GJ, Roopenian DC, Shaw AS. Neonatal FcR expression in bone marrow-derived cells functions to

protect serum IgG from catabolism. *J Immunol*. 2007;179:4580–4588.

6. Jones EA, Waldmann TA. The mechanism of intestinal uptake and transcellular transport of IgG in the neonatal rat. *Gut*. 1971;12:855–856.
7. Cianga P, Cianga C, Cozma L, Ward ES, Carasevici E. The MHC class I related Fc receptor, FcRn, is expressed in the epithelial cells of the human mammary gland. *Hum Immunol*. 2003;64:1152–1159.
8. Dall'Acqua WF, Woods RM, Ward ES, et al. Increasing the affinity of a human IgG1 for the neonatal Fc receptor: biological consequences. *J Immunol*. 2002;169:5171–5180.
9. Waldmann TA, Strober W. Metabolism of immunoglobulins. *Prog Allergy*. 1969;13:1–110.
10. Kim H, Fariss RN, Zhang C, Robinson SB, Thill M, Csaky KG. Mapping of the neonatal Fc receptor in the rodent eye. *Invest Ophthalmol Vis Sci*. 2008;49:2025–2029.
11. McKenzie JA, Fruttiger M, Abraham S, et al. Apelin is required for non-neovascular remodeling in the retina. *Am J Pathol*. 2012;180:399–409.
12. Roopenian DC, Christianson GJ, Sproule TJ, et al. The MHC class I-like IgG receptor controls perinatal IgG transport, IgG homeostasis, and fate of IgG-Fc-coupled drugs. *J Immunol*. 2003;170:3528–3533.
13. Petkova SB, Akilesh S, Sproule TJ, et al. Enhanced half-life of genetically engineered human IgG1 antibodies in a humanized FcRn mouse model: potential application in humorally mediated autoimmune disease. *Int Immunol*. 2006;18:1759–1769.
14. Uhlen M, Oksvold P, Fagerberg L, et al. Towards a knowledge-based Human Protein Atlas. *Nat Biotechnol*. 2010;28:1248–1250.
15. Christianson GJ, Sun VZ, Akilesh S, Pesavento E, Proetzel G, Roopenian DC. Monoclonal antibodies directed against human FcRn and their applications. *MAbs*. 2012;4.
16. Ito D, Imai Y, Ohsawa K, Nakajima K, Fukuuchi Y, Kohsaka S. Microglia-specific localisation of a novel calcium binding protein, Iba1. *Brain Res Mol Brain Res*. 1998;57:1–9.
17. Schlachetzki F, Zhu C, Pardridge WM. Expression of the neonatal Fc receptor (FcRn) at the blood-brain barrier. *J Neurochem*. 2002;81:203–206.
18. Liu X, Ye L, Christianson GJ, Yang JQ, Roopenian DC, Zhu X. NF-kappaB signaling regulates functional expression of the MHC class I-related neonatal Fc receptor for IgG via intronic binding sequences. *J Immunol*. 2007;179:2999–3011.
19. Borvak J, Richardson J, Medesan C, et al. Functional expression of the MHC class I-related receptor, FcRn, in endothelial cells of mice. *Int Immunol*. 1998;10:1289–1298.
20. van BK, van Hagen PM, Bastiaans J, et al. The neonatal Fc receptor is expressed by human retinal pigment epithelial cells and is downregulated by tumour necrosis factor-alpha. *Br J Ophthalmol*. 2011;95:864–868.
21. Qiao SW, Kobayashi K, Johansen FE, et al. Dependence of antibody-mediated presentation of antigen on FcRn. *Proc Natl Acad Sci U S A*. 2008;105:9337–9342.
22. Newman AM, Gallo NB, Hancox LS, et al. Systems-level analysis of age-related macular degeneration reveals global biomarkers and phenotype-specific functional networks. *Genome Med*. 2012;4:16.
23. Cherepanoff S, McMenamin P, Gillies MC, Kettle E, Sarks SH. Bruch's membrane and choroidal macrophages in early and advanced age-related macular degeneration. *Br J Ophthalmol*. 2010;94:918–925.
24. Parmeggiani F, Romano MR, Costagliola C, et al. Mechanism of inflammation in age-related macular degeneration. *Mediators Inflamm*. 2012;2012:546786.
25. Sen DK, Sarin GS, Saha K. Immunoglobulins in human aqueous humour. *Br J Ophthalmol*. 1977;61:216–217.
26. Zhang Y, Pardridge WM. Mediated efflux of IgG molecules from brain to blood across the blood-brain barrier. *J Neuroimmunol*. 2001;114:168–172.
27. Deane R, Sagare A, Hamm K, et al. IgG-assisted age-dependent clearance of Alzheimer's amyloid beta peptide by the blood-brain barrier neonatal Fc receptor. *J Neurosci*. 2005;25:11495–11503.
28. Carneiro AM, Costa R, Falcao MS, et al. Vascular endothelial growth factor plasma levels before and after treatment of neovascular age-related macular degeneration with bevacizumab or ranibizumab. *Acta Ophthalmol*. 2012;90:e25–e30.
29. Davidovic SP, Nikolic SV, Curic NJ, et al. Changes of serum VEGF concentration after intravitreal injection of Avastin in treatment of diabetic retinopathy. *Eur J Ophthalmol*. 2012;22:792–798.
30. Zehetner C, Kirchmair R, Huber S, Kralinger MT, Kieselbach GF. Plasma levels of vascular endothelial growth factor before and after intravitreal injection of bevacizumab, ranibizumab and pegaptanib in patients with age-related macular degeneration, and in patients with diabetic macular oedema. *Br J Ophthalmol*. 2013;97:454–459.
31. Matsuyama K, Ogata N, Matsuoka M, Wada M, Takahashi K, Nishimura T. Plasma levels of vascular endothelial growth factor and pigment epithelium-derived factor before and after intravitreal injection of bevacizumab. *Br J Ophthalmol*. 2010;94:1215–1218.

Investigative Ophthalmology & Visual Science